LIMNOLOGY
and
OCEANOGRAPHY: METHODS

ASLO

Limnol. Oceanogr.: Methods 14, 2016, 456–465

doi: 10.1002/lom3.10104

A surface plasmon resonance system for the underwater detection of domoic acid

Florent Colas,*[1] Marie-Pierre Crassous,[1] Sebastien Laurent,[1] Richard W. Litaker,[2] Emmanuel Rinnert,[1] Erwan Le Gall,[1] Michel Lunven,[1] Laurent Delauney,[1] Chantal Compère[1]

[1]Ifremer Centre de Brest, Technopôle Brest-Iroise, Plouzané, France

[2]National Oceanic and Atmospheric Administration, National Ocean Service, Center for Coastal Fisheries and Habitat Research, Beaufort, North Carolina

Abstract

Over the past decade Surface Plasmon Resonance (SPR) techniques have been applied to the measurement of numerous analytes. In this article, an SPR biosensor system deployed from an oceanographic vessel was used to measure dissolved domoic acid (DA), a common and harmful phycotoxin produced by certain microalgae species belonging to the genus *Pseudo-nitzschia*. During the biosensor deployment, concentrations of *Pseudo-nitzschia* cells were very low over the study area and measured DA concentrations were below detection. However, the in situ operational detection limit of the system was established using calibrated seawater solutions spiked with DA. The system could detect the toxin at concentrations as low as 0.1 ng mL^{-1} and presented a linear dynamic range from 0.1 ng mL^{-1} to 2.0 ng mL^{-1}. This sensor showed promise for in situ detection of DA.

Introduction

Over the past few decades there has been a growing recognition of the crucial ecological and socio economic importance of the oceans and just how little is known about the basic biological and physical processes that govern their health. Given the vast size of the oceans, and reduced funding for ship operations, the only way to obtain the crucial information required to address these significant data gaps is through the development of automated sensors (temperature, salinity, nutrients, pollutants, biotoxins, and various organisms) which can be deployed on autonomous vehicles or platforms at significantly lower costs. The development of these sensor systems, however, is still in its infancy with most analyses still needing to be performed in the laboratory using complex analytical equipment. These in-laboratory systems require collection of seawater samples prior to analyses making them more expensive and time-consuming to perform. Further, the resulting data sets are typically less spatially and temporally resolved than those collected from autonomous vehicles and platforms. Consequently, there is a great impetus for developing the next generation of automated sensors.

One of the most promising technologies currently being adapted for this purpose is Surface Plasmon Resonance (SPR) (Melendez et al. 1996; Naimushin et al. 2003; Kawazumi et al. 2005). Díaz-Herrera et al. (2006) reported an in situ SPR system using special optical fibers for measuring salinity of seawater using the determination of refractive index. The sensor was then deployed on a pelagic profiler and successfully acquired salinity profiles. Kim et al. (2011), presented a similar optical fiber based SPR system for in situ measurement of refractive index and deployed it in 2013 in deep water (Kim et al. 2013). These experiments proved that SPR was a technology mature enough to be implemented in harsh environments such as oceans. However, no in situ SPR biosensor has been deployed to date. In contrast, numerous quantitative laboratory-based SPR detection systems have been developed for various marine molecules in particular the biotoxin domoic acid (DA) (Lotierzo et al. 2004; Yu et al. 2005; Le Berre and Kane 2006; Traynor et al. 2006; Stevens et al. 2007; Doucette et al. 2009; Campbell et al. 2011). Currently, the most sensitive laboratory SPR assay can detect DA as low as 0.1 μg L^{-1} in a shellfish extract (Yu et al. 2005).

DA is produced by certain microalgal species belonging to the genus *Pseudo-nitzschia* and by *Nitzschia navis-varingica*. This toxin is readily concentrated by shellfish as they filter feed (Bejarano et al. 2008). Consumption of tainted shellfish can cause amnesic shellfish poisoning and potential damage to the hippocampus and amygdaloid nucleus regions of the brain.

The production of DA by *Pseudo-nitzschia* species is a complex process that is not fully understood. Nutritional

*Correspondence: florent.colas@ifremer.fr

physiology studies demonstrated that the stress of macronutrient (N, P, or Si) limitation plays a key role in the production of DA by the cells (reviewed by Trainer et al. 2012). For instance, laboratory studies with *Pseudo-nitzschia* multiseries showed that the production of the toxin becomes detectable only when Si or P limitation slows down the exponential growth rate (Bates 1998). Conversely, Auro (2007) demonstrated that cells of *P. cupisdata* contained more DA during the exponential growth than in the stationary phase when nitrogen was the limiting macronutrient. There is then no straightforward relationship between the DA concentration and number of cells. In addition, the release of the toxin by the cells is still subject to investigations. Evidence indicates that DA chelates iron and copper and that it plays a role in iron acquisition when concentrations are limiting the growth or in the detoxification of copper (Trainer et al. 2012). Maldonado et al. (2002) showed that 95% of the DA can be released in some metal stressed conditions.

Trainer et al. (2007) reported that in a closed area of Washington state inland waters where cell concentrations ranged from 3,000 cells L^{-1} to 500,000 cells L^{-1}, dissolved DA ranged from 0.06 ng mL^{-1} to 3 ng mL^{-1}. The amount of dissolved DA was much larger than the particulate DA. In contrast, in 2004 a bloom of nearly monospecific *Pseudo-nitzschia cupisdata* off the coast of the Washington state yielded concentrations of particulate DA 10 times greater than the dissolved DA from cell concentrations of about 6 10^6 L^{-1} (Trainer et al. 2009). In this study, iron limitation appeared to play a role in controlling the DA production. The mechanisms regulating DA production are clearly complex and there is still a need for investigating the *Pseudo-nitzschia* physiology and role of the DA in coastal ecosystems.

This study focused on developing a SPR system for real-time in situ quantification of DA. As a first step, we concentrated on measuring dissolved DA. The requirement to measure only dissolved DA simplifies the design of the sample processing system, significantly lowering construction and deployment costs compared to other systems which require a module to collect and extract DA from the cells. To our knowledge, no other system is dedicated to performing such an assay and we believe that such a tool will be useful in executing ecological and physiological studies and understanding the role of dissolved DA in complex ecosystems. The eventual goal is to establish how well dissolved DA reliably indicates when levels of *Pseudo-nitzschia* cells are present.

This article reports the results from the initial deployment of the underwater dissolved DA SPR-based detection system during a cruise in 25 June 2011, in the Bay of Vilaine, a location where blooms of toxic *Pseudo-nitzschia* spp. are known to occur in the spring. The sensitivity of the system is sufficient to detect concentrations of DA as low as 0.1 ng mL^{-1} with a dynamic range of 0.1-1.0 ng mL^{-1}.

Material and procedures

The surface plasmon resonance transducer

The basic principles underlying SPR are reviewed in (Homola 2008). The specific SPR transducer used in this study is based on the spectral interrogation principle (Homola 2006). It consists of two modules. The first encloses the light source, the spectrophotometer and some electronics while the second, called the optode, contains the optics and two SPR chips, one for each measurement channel (Fig. 1).

The light from a tungsten halogen lamp (HL1000, Mikropack GmbH, Germany) is focused onto a multimode optical fiber coupler then routed through two optical fibers to the optode. Each light beam coming out of a fiber is collimated by an achromat doublet of 4.5 mm focal length and then passed through a linear polarizer (Fig. 2). Then the beam is first reflected onto the N-F2 prism by Total Internal Reflection (TIR), second onto one of the SPR chip and finally on the prism by TIR again. A second achromat doublet focuses light into an optical fiber connected to the spectrophotometer. This consists of a Carpenter-based axial spectrometer (Jobin Yvon®, France) equipped with a 16-bits CCD (Charge Coupled Device) camera (ST3200ME, SBIG Astronomical Instruments, U.S.A.), driven by an embedded computer (Wafer C400, IEI Technology Corporation, Taiwan). The spectrophotometer works in the near IR range from 600 nm to 950 nm.

The SPR is an N-F2 glass slide chip (N-F2, Schott, Switzerland) coated with a 50 nm thick gold film. It has a 10 mm-diameter and is 1 mm-thick. The chip is then placed against the prism after applying a drop of refractive index matching liquid in between. This configuration makes it easy to replace the SPR chip as needed and also has the advantage of eliminating any alignment issues.

To accurately calculate the position of the SPR absorption band, called the dip hereafter, it is necessary to normalize the reflected spectrum by a reference spectrum that takes into account the different spectral transmittance of the optical systems without surface plasmon absorption. To do so, the reflected spectrum was measured with ethanol in the flow cell. Because of the high refractive index of ethanol (1.36) compared to that of water (1.33), the surface plasmons are generated out of the range of the spectrophotometer. This enabled us to avoid traditional normalization by s-polarized light that would require rotating the polarizer by 90° and the integration of an automatic rotation stage.

The SPR sensor was linked to the boat by a submarine power cable that provides 24 V to the system and a submarine Ethernet cable. The latter enabled real-time control of the system using a virtual-network-computing software (UltraVNC, FreeWare). This configuration is close to the one reported by Cahill et al. (1997).

Compartmentalizing the optode and the light source/spectrophotometer/electronics into separate modules

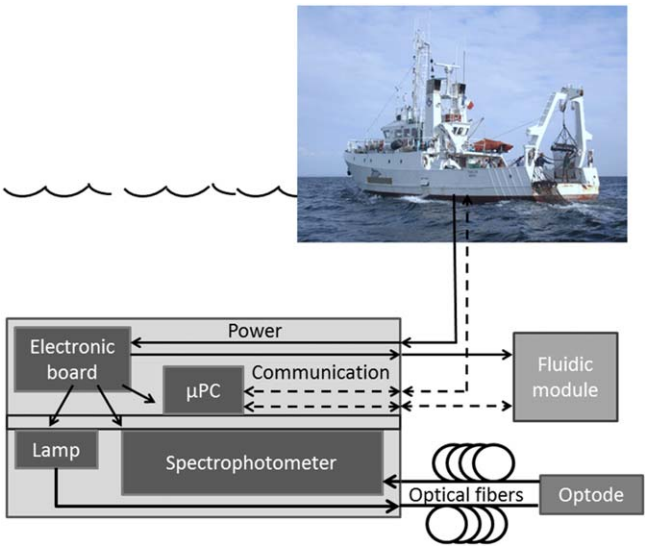

Fig. 1. The underwater SPR system is linked to the boat by an Ethernet cable and a power cable. The big container contains an electronic board that supplies power to the lamp, the spectrophotometer, the fluidic module and an embedded computer (μPC). Light from the lamp is brought to the optode, reflected onto the SPR chip and the resultant light emerging from the prism carried to the spectrophotometer via optical fibers. The computer analyses the signal from the spectrophotometer, communicates the data to the boat and drives the fluidic module by a RS232 communication protocol. The sample is pumped through a filter and brought to the fluidic module by PTFE manifolds.

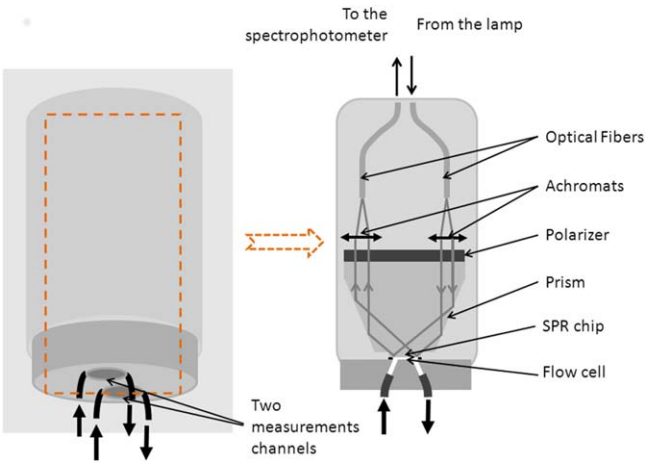

Fig. 2. The optode. The view on the left shows the two measurement channels. The scheme on the right presents the optical path through one measurement channel. The light out of the incoming optical fibers is collimated by a short focal length lens, linearly polarized. It is then reflected on the SPR chip and launched into an optical fiber connected to the spectrophotometer.

enhanced the durability of the system. It also allowed the optode to be easily coupled to other equipment such as the fluidic module that injects processed seawater samples. In particular, a flow cell made of PolyEtherEtherKetone (PEEK) can be adapted to the optode and connected to the fluidic module by manifolds.

The SPR chip functionalization

Since DA is a small molecule of only 311 Da and the SPR signal shift is proportional to added quantities of matter, a direct detection would not be sensitive enough to detect the toxin at concentration lower than few ng mL^{-1} (Lotierzo et al. 2004; Yu et al. 2005; Le Berre and Kane 2006; Traynor et al. 2006; Stevens et al. 2007; Doucette et al. 2009; Campbell et al. 2011). To circumvent this limitation, an alternative method relies on an indirect detection such as an inhibition assay format (Dostálek et al. 2006). Briefly, a known amount of DA is anchored to a SPR chip during the functionalization step. Then, the seawater sample to be analyzed is mixed with a known quantity of anti-DA antibodies (Ab) that binds the toxin during a defined incubation time. Hereafter the mixture is kept in contact with the SPR chip. In seawater samples without any DA, all Ab in the mixture remains free to bind the DA attached to the chip. When free DA is present in the sample there are fewer Ab molecules available to bind the immobilized DA. Quantitation of DA in the sample becomes possible as the initial concentration of the toxin is correlated with the remaining fraction of free anti-DA Ab that binds to the DA immobilized on the chip.

The SPR chips, to which DA was attached, were produced following the protocol developed by Yu et al. (2005) and Ab produced by Mercury Science (Durham, North Carolina, U.S.A.). Slides were first immersed in a solution of thiolated alkyl- PolyEthylene Glycol (PEG) modified with a NH_2 terminal group (Prochimia). During this step, a Self-Assembled Monolayer formed on the gold surface. The DA molecule contains three carboxylic groups. They were activated with a N-HydroxySuccinimid/(1-ethyl-3-(3-dimethylaminopropyl) carbodiimide) mixture and the activated DA was then deposited on the SPR chip. Each of these activated esters reacted in a random manner with the primary amine function of the modified PEG to form a stable amide bond.

Fluidic module

The fluidic module was first developed for colorimetric assays of different chemical compounds (Vuillemin et al. 2009). It consists of eight electrovalves and three peristaltic pumps that can turn clockwise or counter-clockwise and whose rotation speed can be adjusted. The reagents are stored in plastic bags and linked to the pumps, the valves, and the SPR system by polytetrafluoroethylene (PTFE) manifolds. The mixing cell is a PTFE manifold that had been specially shaped to form circumvolutions to ensure homogeneous mixture of the reagents (Fig. 3).

The fluidic module is designed to perform an inhibition assay. First, the seawater sample is pumped through a 0.2 μm diameter pore Minisart syringe filter (Sartorius, Bohemia, New York, U.S.A.). Second, the filtrate and the antibody

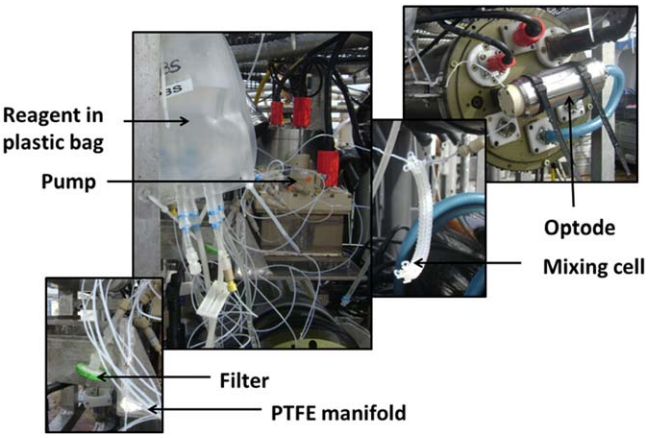

Fig. 3. The fluidic module composed of the admission filter, PTFE manifolds, plastic bags containing the reagents, the pumps and valves, the mixing cell and the flow cell of the optode.

solution are injected inside a mixing cell during a 15 min period. Once equilibrated, this solution is injected in the flow cell over 15 min and the λ_{SPR} change measured. To regenerate the sensor surface for the next assay, the SPR cell is rinsed successively with phosphate buffered saline (PBS), 0.1 mM NaOH and then PBS. The output from the spectrophotometer is continuously recorded during the measurement and regeneration steps.

Underwater characterization of the transducer

The aim of this set of experiments was to measure the sensitivity and the resolution of the SPR sensor with regard to refractive index at 0, 10 m and 20 m ocean depth from an oceanographic vessel during the oceanographic cruise NITTEK (Iroise Sea, 16 December 2009). Sucrose solutions were used to optically characterize the transducer, knowing that the refractive index of solutions of this compound is proportional to its mass concentration. Sucrose was selected for its chemical stability and inertia against a gold surface. Solutions of 0.1%, 0.2%, 0.5%, and 1% sucrose were stored in plastic bags attached to the structure. The whole system was mounted onto a metallic frame along with other equipment such as conductivity, temperature, depth sensors (SBE25 CTD probe, Sea Bird Electronics, Bellevue, Washington, DC, U.S.A.).

Domoic acid assay optimization

The inhibition assay was developed according to the work of Yu et al. (2005). For the DA assay to be successful it had to be capable of detecting toxin at a concentration of 0.1 ng mL^{-1} in seawater. To detect small amounts of DA, the concentration of Ab needed to be optimized. When the antibody concentration was too high the binding with the dissolved DA was not measurable since most of the free Ab, bound to the surface, saturated the reactive sites quickly. When the antibody concentration was too low, the binding of the Ab on the surface was not detected because the amount of Ab on the surface was too small to be detected by SPR.

To get an adequate concentration range of Ab for assay optimization, we had to consider, first, that one IgG molecule was able to trap up to two DA molecules in seawater solution. Second, the two binding sites had to be occupied by DA from the sample to become nonreactive against the DA sensor surface. Third, given the nanomolar affinity observed in standard buffers (Litaker et al. 2008) and the expected Ab concentrations needed for the inhibition protocol, we postulated the reaction was stoichiometric. Thus, to detect DA at concentration up to 5 ng mL^{-1}, we needed to have a final Ab concentration of at least 1.2 μg mL^{-1}, assuming an Ab molecular weight of 150 kDa.

To determine the optimal antibody concentration Ab solutions of concentrations (C_0) ranging from 0.4 μg mL^{-1} to 3.2 μg mL^{-1} were injected into the flow cell. Then the response curve of the sensor was acquired with PBS and artificial seawater solutions spiked with DA at concentrations ranging from 0 ng mL^{-1} to 10 ng mL^{-1}.

Ocean deployment

The system was mounted on a pelagic profiler. Our system was combined with an SBE25 CTD probe (Sea Bird Electronics, Bellevue, Washington, DC, U.S.A.), a fluorometer (Seapoint Sensors Inc., Brentwood, New Hampshire, U.S.A.), a laser Particle Size Analyzer (Gentien et al. 1995) for measuring the size of particles in seawater and an innovative imaging system: the L'Institut Français de Recherche pour l'Exploitation de la Mer (Ifremer) in situ Video-Fluo-Analyzer (Lunven et al. 2012) for imaging the phytoplankton cells. Then, when the presence of *Pseudo-nitzschia* cells could be assumed from the in situ image analysis, seawater samples were analyzed with our system. Prior to the toxin detection, calibration was performed with seawater spiked with DA to compare the response curve of our sensor during lab and in situ measurements.

Assessment

Underwater characterization of the transducer

The sucrose solutions of increasing mass concentration were sequentially injected into the flow cell and the corresponding dip shifts were quantified. To limit measurement bias (i.e., because of drifting baseline), the flow cell was rinsed in between samples with deionized water. This experiment was carried out three times: on the deck, at 10 m and 20 m depth. Figure 4 shows a typical plot of the SPR wavelength (λ_{SPR}) over time, hereafter called a sensorgram. The inset on Fig. 4 shows a graph of λ_{SPR} shifts ($\Delta\lambda_{SPR}$) obtained from the previous sensorgams with regard to the refractive index measured on the deck, at 10 m and 20 m ocean depth.

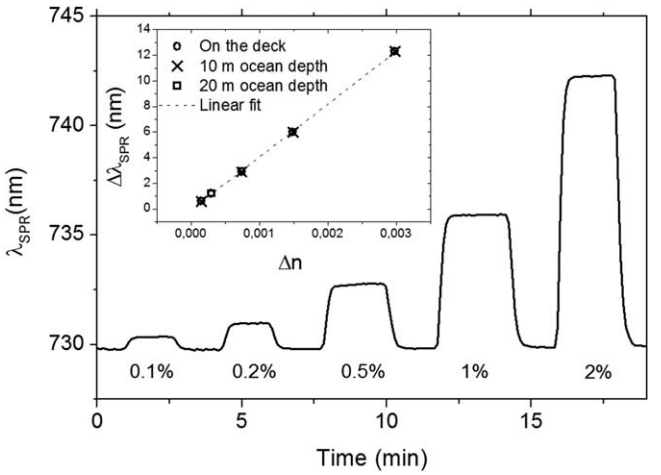

Fig. 4. Sensorgram of the injection of the sucrose solutions at 10 m ocean depth. The inset represents the sensitivity of the sensor to the refractive index shift. It is defined as the derivative of the wavelength shift with regards to the refractive index.

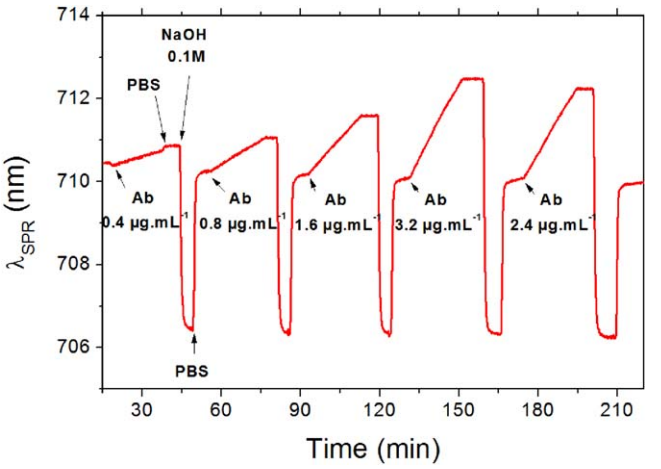

Fig. 5. Sensorgrams of the injections of solution of concentrations of Ab ranging from 0.4 μg mL^{-1} to 3.2 μg mL^{-1}.

In all three cases, the sensor responses are very similar. The sensitivity to refractive index changes (S_i) is defined as the derivative of the λ_{SPR} shift with regards to the refractive index change. In the three cases, S_i was very similar (less than 3% difference) and was estimated to about 4100 nm/RIU by a linear fit of the data reported on Fig. 5. This result is consistent with numerical simulations based on the Rouard method (Lecaruyer et al. 2006), which led to a theoretical sensitivity of 4400 nm (data not shown).

The surface density change ($\Delta\Gamma$) can be related to $\Delta\lambda_{SPR}$ by (Maillart 2004):

$$\Delta\Gamma = \frac{\Delta\lambda_{SPR} L}{S_i \frac{\delta n}{\delta C}} \quad (1)$$

where L is the plasmon penetration depth in the liquid and $\partial n/\partial C$ the derivative of the refractive index change with regards to the concentration of the target molecule. The former can be estimated to 75 nm in that configuration (Maillart 2004) and the latter to 0.19 cm^3 g^{-1} for Ab (Karlsson et al. 1991). Then,

$$\Delta\Gamma \approx 10\Delta\lambda_{SPR}. \quad (2)$$

where $\Delta\Gamma$ is in ng cm^{-2}, $\Delta\lambda_{SPR}$ in nm. The smallest change in mass surface density that can be detected is estimated to be 300 pg cm^{-2} considering the lowest detectable $\Delta\lambda_{SPR}$ is three times the standard deviation of the baseline noise. This value is consistent with other systems which were capable of detecting biomolecules (Piliarik and Homola. 2006).

It is worth noting that there is no active temperature regulation. First, the ocean thermal inertia will avoid rapid temperature change over the duration of the assay carried out at a fixed depth. Also, in the second measurement channel, referred to as the reference channel, PBS solution is circulated during the assay. Signal changes related to temperature affect both channels. Thermal drifts are measured by the reference channel and the signal of the measurement channel can then be corrected if necessary.

Domoic acid assay optimization

Ab solutions of concentrations (C_0) ranging from 0.4 μg mL^{-1} to 3.2 μg mL^{-1} were injected into the flow cell and between each of these injections, the flow cell was rinsed with PBS, regenerated with NaOH (0.1M) and then rinsed with PBS. Figure 5 shows the sensorgram of this experiment. The reaction of anti-DA Ab on the surface resulted in a quasilinear increase of λ_{SPR} with time. During the PBS rinsing phase, the signal remained constant, which indicated a strong binding of the Ab to the functionalized chip and no nonspecific adsorption.

One can expect that λ_{SPR} shifts will continue to increase after a 15 min-injection. Nevertheless a longer injection time would cause a longer assay time, which is not compatible with marine system deployment. The concentration of Ab for the assay was set to 1.6 μg mL^{-1} to work with a high signal-to-noise ratio.

The response curve of our sensor was then determined for the toxin assay in PBS. Eight solutions spiked with DA at different concentrations (100 ng mL^{-1}, 10 ng mL^{-1}, 5 ng mL^{-1}, 1 ng mL^{-1}, 0.8 ng mL^{-1}, 0.5 ng mL^{-1}, 0.1 ng mL^{-1}, and 0 ng mL^{-1}) were prepared. One mL of each was incubated with the Ab for 15 min before injection at room temperature. The SPR chip was regenerated between each of the injection with NaOH solutions (0.1M). Figure 6 presents a graph of the normalized SPR wavelength shift rate η_n, defined as:

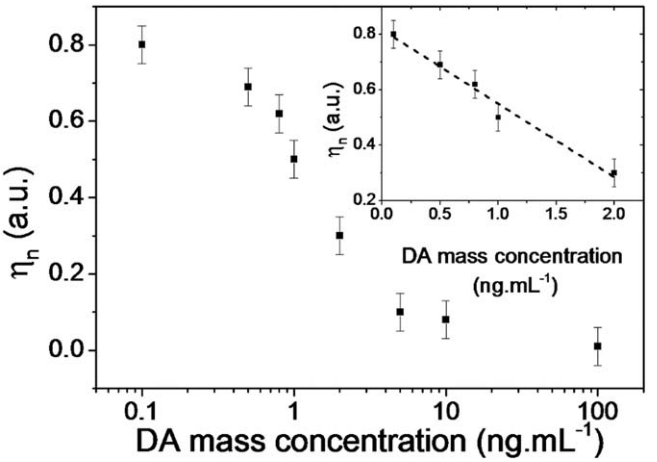

Fig. 6. Response curve of the biosensor for PBS solutions

$$\eta_n([\mathrm{DA}]) = \frac{\eta([\mathrm{DA}])}{\eta(0)} \quad (3)$$

The response curve of the biosensor presents a shape typical of inhibition assay.

As expected, for concentrations higher than 5 ng mL^{-1} the λ_{SPR} shift rate change was insignificant. The inset on Fig. 6 depicts the same data but in a different range (0–2 ng mL^{-1} along a linear scale). Over this range, the biosensor response was linear and indicated an EC_{50} (effective concentration to reach 50% of the response) value of 1.25 ng mL of DA. With an Ab concentration of 1.6 μg mL^{-1}, the limit of detection (LOD) was estimated to 0.1 ng mL^{-1}, by taking into account the uncertainty of the determination of the shift rate.

The sensitivity and the dynamic range of that SPR DA assay compares well with previously published data using the ELISA format (Litaker et al. 2008). Note that if higher concentrations have to be assayed, the Ab concentration must be increased but at the expense of sensitivity. It is worth noting that the whole measurement process (detection and regeneration) can be performed at least 10 times without a significant loss of sensitivity. The Ab had lower affinity for the DA when working with seawater samples (data not shown) mainly because of the high ionic strength of the latter medium and the greater contribution of electrostatic forces in the Ab binding mechanism to the toxin DA. To alleviate this lack of sensitivity, the concentration of Ab was increased slightly to 2 μg mL^{-1}. In addition, it was decided that during the assay, the seawater sample would be mixed with the same volume of Ab solutions. On the one hand, the sample is diluted by a factor 2. On the other hand, it diminishes the ionic strength of the mixture and favors the reaction of the Ab with the DA.

The graph in Fig. 7 is the response curve of the biosensor in a linear scale. It represents η_n with regards to the DA

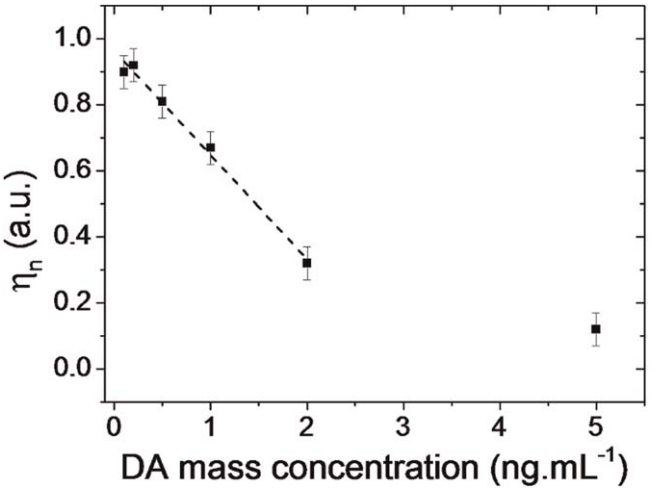

Fig. 7. Response curve of the SPR sensor with seawater samples

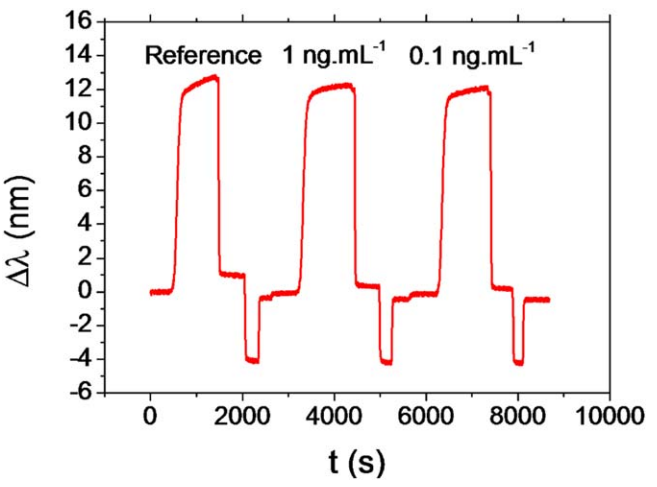

Fig. 8. Sensorgram of the injection of calibration solutions during underwater experiments

concentration for seven seawater samples (0 ng mL^{-1}, 0.1 ng mL^{-1}, 0.2 ng mL^{-1}, 0.5 ng mL^{-1}, 1 ng mL^{-1}, 2 ng mL^{-1}, and 5 ng mL^{-1}). As previously, the dynamic range is still relatively narrow but it enabled us to achieve a detection limit as low as 0.1 ng mL^{-1}. The linear part of the sensor response goes to about 2 ng mL^{-1}. Then, the diminution of the ionic strength of the mixture and the increase of the Ab concentration enabled us to reach a similar sensitivity of the assay in PBS as attested by an EC_{50} of 1.5 ng mL^{-1}, only 20% larger than previously.

Ocean deployment

During the oceanographic cruise, three seawater solutions with DA at 0, 0.1 ng mL^{-1} and 1 ng mL^{-1} were first injected from a reservoir for calibration purposes. These concentrations were chosen because this is the linear response range of the sensor. They also served as a control in case the waters

Table 1. Comparison of the response of the sensor in the laboratory and underwater

DA mass concentration (ng mL^{-1})	η_n in the laboratory	η_n underwater
0.1	0.91	0.42
1	0.66	0.3

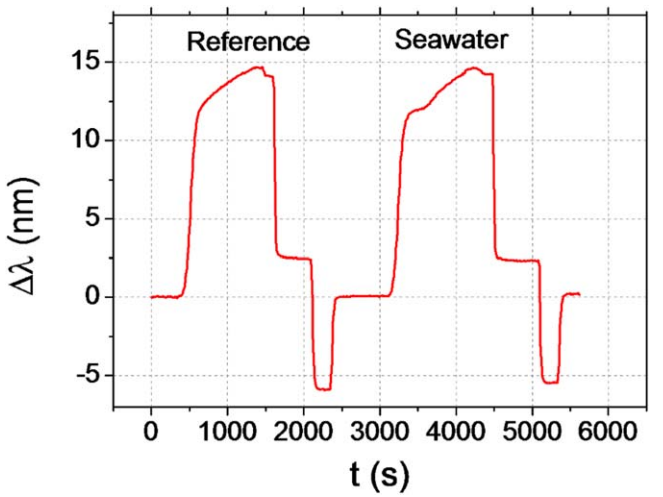

Fig. 9. Sensorgramm of the underwater analysis of seawater

being sampled contained minimal concentrations of *Pseudo-nitzschia*. The sensorgram of those calibration injections can be seen in Fig. 8. As expected, the higher the DA concentration, the slower the signal increases. However, compared to a lab environment, overall performance for the assay was modified as reported in Table 1. Underwater, concentrations as low as 0.1 ng mL^{-1} led to a 58% decrease of the signal compared to seawater reference without DA, while in the lab only a 10% change was measured.

Once the sensor was demonstrated to be operational, seawater samples were analyzed with the sensors on the pelagic profiler. Unfortunately, during this period, we could not detect a significant number of cells of *Pseudo-nitzschia* spp. This observation was verified by microscopic examination of water samples collected at different depths. We analyzed a seawater sample anyway. The corresponding sensorgrams are shown in Fig. 9. The slope of the linear increase of the reference and the seawater sample showed no significant change. Only a 3% variation was measured by fitting a line to the linear part of the graph corresponding to the Ab reaction on the SPR chip. The correlation coefficients R^2 were 0.994 and 0.993 for the reference and the sample, respectively. We then got a $\eta_n = 1.02 \pm 0.02$, the error being estimated from the fit.

Domoic acid toxin was not present at a concentration higher than 0.1 ng mL^{-1} in the seawater at this time and location. Such a conclusion was confirmed afterwards by the results of a standard microscopic cell counting method (Utermöhl 1931) which showed less than 10,000 L^{-1} *Pseudo-nitzschia* spp. were present in all the samples examined. These cell concentrations were insufficient to produce measurable levels of DA. Hence, the low DA concentrations measured during the cruise are in accordance with the low number of *Pseudo-nitzschia* spp. cells in the phytoplankton samples taken in the stations. Moreover the phytoplankton counts provided by the Ifremer survey network (REPHY) over a one-month period before the cruise confirm a very low abundance of *Pseudo-nitzschia* spp. cells in the study area with abundances lower than the alert threshold for the DA producer species.

Discussion

The SPR biosensor developed and test-deployed in this study is capable of measuring free DA in a seawater matrix over a range of 0.1–2 ng mL^{-1} (Table 1). This sensor shows promise for detection of dissolved DA in seawater in a field deployment. This sensitivity level should be sufficient to detect dissolved DA at levels present during toxic *Pseudo-nitzschia* blooms (Trainer et al. 2007). Consequently, remotely deployed platforms employing this sensor system could successfully detect the onset of toxic PN blooms.

As far as we know, the only other *in situ* system reported for DA detection is the Environmental Sampler Processor (Doucette et al. 2009). This well documented system was proven efficient for monitoring harmful algae as it can detect algal species in addition to phycotoxins. The DA assay they reported is two orders of magnitude less sensitive than our SPR instrument. However, the ESP can assay the particulate DA (Doucette et al. 2009) because it is able to collect the cells on a filter and then extract the toxin, which might be an efficient way of detecting a harmful algal bloom event. Clearly, these two systems can be very complementary.

Comments and recommendations

Our optimization experiment led us to explore several buffer and temperature conditions. Ionic strength was found to be particularly important in modulating affinity of Ab for the biotoxin and the overall sensitivity of the assay. Considering standard seawater (U.S. Department of Energy [DOE] 1994) as an approximation, an ionic strength of 704 mM was calculated, which is four times higher than that of PBS buffer. Consequently, we recommended that samples be partially diluted with PBS to reduce the ionic strength of the sample and ensure optimal performance.

To save power in the current iteration of the SPR biosensor, the solutions were not temperature controlled. All field experiments were carried out at 13°C as compared to 20°C in the laboratory. This temperature difference caused a significant shift in the overall sensitivity of the assay (Table 1).

This behavior has been previously reported (Colas et al. 2010). We hypothesize that the performance difference comes from a positive balance between a kinetic speed decrease together with an antibody affinity change over temperature as is predicted by the Arrhenius law and the van't Hoff equation for protein–protein interactions (Navratilova et al. 2007; de Mol and Fische 2008). This means that either the reactions have to be temperature controlled or a standard curve must be run to recalibrate the instrument for the prevailing water temperatures.

A logical future modification of our SPR biosensor would be incorporation of additional toxins. Technologies currently being developed which allow robust spectral multidetection (e.g., Sereda et al. 2014) may pave the way to in situ multianalyte detection. Campbell et al. (2011) for example, reported a laboratory SPR instrument capable of simultaneously monitoring saxitoxin, okadaic acid, and DA in seawater samples (McNamee et al. 2013). However, the lower limit of detection for DA was an order of magnitude higher than our system and could not be used for direct detection of dissolved DA in seawater.

Enhancing the sensitivity of these systems to detect the low levels of dissolved toxin which occur in the water column would require an increased signal-to-noise (S:N) ratio. One approach for boosting the S:N ratio is to increase surface binding capacity using polymers like dextrans. This forms a brush-like network extending 100 nm to 200 nm to the flow cell, increasing the accessibility of the probe. We would then be able to work with lower Ab concentrations, which would lead to a lower limit of detection. Another recent and interesting approach to increasing sensitivity is to use Ab attached to gold nanoparticles (Dribek et al. 2014). Measurements have shown that the SPR signal induced by the reaction of the gold labeled Ab on the chip is much larger than what can be achieved with nonlabeled antibodies. It would then be possible to work with lower antibody concentrations.

Even though our system demonstrates very good performances, the relative standard deviation of the measurements is about 15%, which is two to three times greater than with chemical methods (Wang et al. 2007; Devez and Delmas 2013).

Conclusion

In this article, a SPR transducer for submarine experiments is presented and characterized. Its sensitivity enables accurate measurement of the refractive index from a boat or at different ocean depths. An inhibition assay for detecting a biotoxin in a seawater matrix was then developed and assessed during shipboard experiments. These experiments showed the high potential of SPR techniques for environmental application, even in the harsh marine environment. Although the relationship between *Pseudo-nitzschia* cell and toxin concentrations in seawater in still unclear, we believe the biosensor reported in this article can be used as a new tool to investigate the complex process of production and release of DA in coastal waters.

References

Auro, M. E. 2007. Nitrogen dynamics and toxicity of the pennate diatom *Pseudo-nitzschia cuspidata*: A field and laboratory study. Masters thesis. San Francisco State Univ.

Bates, S. S. 1998. Ecophysiology and metabolism of ASP toxin production, p. 405–426. *In* D. M. Anderson, A. D. Cembella, and G. M. Hallegraeff [eds.], Physiological ecology of harmful algal blooms. Springer Verlag.

Bejarano, A. C., F. M. van Dola, F. M. Gulland, T. K. Rowles, and L. H. Schwacke. 2008. Production and toxicity of the marine biotoxin domoic acid and its effects on wildlife: A review. Hum. Ecol. Risk Assess. **14**: 544–567. doi:10.1080/10807030802074220

Cahill, C. P., K. S Johnston, and S. S. Yee. 1997. A surface plasmon resonance sensor probe based on retro-reflection. Sens. Actuators B **45**: 161–166. doi:10.1016/S0925-4005(97)00290-6

Campbell, K., and others. 2011. Use of a novel micro-fluidic device to create arrays for multiplex analysis of large and small molecular weight compounds by surface plasmon resonance. Biosens. Bioelectron. **26**: 3029–3036.

Colas, F., M.-P. Crassous, W. Litaker, S. Laurent, E. Rinnert, C. Compère, and P. Gentien. 2010. New approach for direct detection of domoic acid, p. 206–208. *In* P. Pagou and G.Hallegraeff [eds.], Proceedings of the 14th International Conference on Harmful Algae. International Society for the Study of Harmful Algae and Intergovernmental Oceanographic Commission of UNESCO.

de Mol, N. J., and M. J. E. Fische. 2008. Kinetic and thermodynamic analysis of ligand–receptor interactions: SPR applications in drug development, p. 123–172. *In* R. B. M. Schasfoort and A. J Tudos [eds.], Handbook of surface plasmon resonance. The Royal Society of Chemistry.

Devez, A., and D. Delmas. 2013. Selective liquid chromatographic determination of trace domoic acid in seawater and phytoplankton: Improvement using the o-phthaldialdehyde/9-fluorenylmethylchloroformate derivatization. Limnol. Oceanogr.: Methods **11**: 327–336.doi:10.4319/lom.2013.11.327

Díaz-Herrera, N., O. Esteban, M. C. Navarrete, M. Lehaitre, and A. González-Cano. 2006. *In situ* salinity measurements in seawater with a fiber-optic probe. Meas. Sci. Technol. **17**: 2227–2232.

Dostálek, J., J. Ladd, S. Jiang, and J. Homola. 2006. SPR biosensors for detection of biological and chemical analytes, p. 177–190. *In* J. Homola and O. S. Wolfbeis [eds.], Surface plasmon resonance based sensors. Springer.

Doucette, G., and others. 2009. Remote, subsurface detection of the algal toxin domoic acid onboard the

environmental sample processor: Assay development and field trials. Harmful Algae **8**: 880–888. doi:10.1016/j.hal.2009.04.006

Dribek, M., and others. 2014. Organometallic nanoprobe to enhance optical response on the polycyclic aromatic hydrocarbon benzo[a]pyrene immunoassay using SERS technology. Environ. Sci. Pollut. Res. 1–7. doi:10.1007/s11356-014-3384-8

Gentien, P., M. Lunven, M. Lehaitre, and J. L. Duvent. 1995. *In situ* depth profiling of particles sizes. Deep Sea Res. Part I **42**: 1297–1312. doi:10.1016/0967-0637(95)00058-E

Homola, J. 2006. Electromagnetic theory of surface plasmons, p. 3–44. *In* J. Homola and O. S. Wolfbeis [eds.], Surface plasmon resonance based sensors. Springer.

Homola, J. 2008. Surface plasmon resonance sensors for detection of chemical and biological species. Chem. Rev. **108**: 462–493.doi:10.1021/cr068107d

Karlsson, R., A. Michaelsson, and L. Mattsson. 1991. Kinetic analysis of monoclonal antibody-antigen interactions with a new biosensor based analytical system. J. Immunol. Methods **145**: 229–240.doi:10.1016/0022-1759(91)90331-9

Kawazumi, H., K. Gobi, K. Ogino, H. Maeda, and N. Miura. 2005. Compact surface plasmon resonance (SPR) immunosensor using multichannel for simultaneous detection of small molecule compounds. Sens. Actuators B **108**: 791–796.doi:10.1016/j.snb.2004.11.069

Kim, Y.-C., J. A. Cramer, and K. S. Booksh. 2011. Investigation of a fiber optic surface plasmon spectroscopy in conjunction with conductivity as an *in situ* method for simultaneously monitoring changes in dissolved organic carbon and salinity in coastal waters. Analyst **136**: 4350–4356. doi:10.1039/c1an15085e

Kim,Y.-C., and others. 2013. Investigation of in situ surface plasmon resonance spectroscopy for environmental monitoring in and around deep-sea hydrothermal vents. Anal. Lett. **46**: 1607–1617. doi:10.1080/00032719.2012.757701

Le Berre, M., and M. Kane. 2006. Biosensor based assay for domoic acid: Comparison of performance using polyclonal, monoclonal, and recombinant antibodies. Anal. Lett. **39**: 1587–1598. doi:10.1080/00032710600713297

Lecaruyer, P., E. Maillart, M. Canva, and J. Rolland. 2006. Generalization of the Rouard method to an absorbing thin-film stack and application to surface plasmon resonance. Appl. Opt. **45**: 8419–8423. doi:10.1364/AO.45.008419

Litaker, R. W., and others. 2008. Rapid enzyme-linked immunosorbent assay for detection of the algal toxin domoic acid. J. Shellfish Res. **27**: 1301–1310. doi:10.2983/0730-8000-27.5.1301

Lotierzo, M., and others. 2004. Surface plasmon resonance sensor for domoic acid based on grafted imprinted polymer. Biosens. Bioelectron. **20**: 145–152. doi:10.1016/j.bios.2004.01.032

Lunven, M., and others. 2012. *In situ* video and fluorescence analysis (VFA) of marine particles: Applications to phytoplankton ecological studies. Limnol. Oceanogr.: Methods **10**: 807–823.

Maillart, E. 2004. Imagerie par résonance des plasmons de surface pour l'analyse simultanée de multiples interactions biomoléculaires en temps réel. Ph.D. thesis. Univ. Paris.

Maldonado, M. T., M. P. Hughes, E. L. Rue, and M. L. Wells. 2002. The effect of Fe and Cu on growth and domoic acid production by *Pseudo-nitzschia multiseries* and *Pseudo-nitzschia australis*. Limnol. Oceanogr. **47**: 515–526. doi:10.4319/lo.2002.47.2.0515

McNamee, S., C. Elliott, P. Delahaut, and K. Campbell. 2013. Multiplex biotoxin surface plasmon resonance method for marine biotoxins in algal and seawater samples. Environ. Sci. Pollut. Res. **20**: 6794–6807. doi:10.1007/s11356-012-1329-7

Melendez, J., and others. 1996. A commercial solution for surface plasmon sensing. Sens. Actuators B **35**: 212–216. doi:10.1016/S0925-4005(97)80057-3

Naimushin, A. N., S. D. Soelberg, D. U. Bartholomew, J. L. Elkind, and C. E. Furlong. 2003. A portable surface plasmon resonance (SPR) sensor system with temperature regulation. Sens. Actuators B **96**: 253–260. doi:10.1016/S0925-4005(03)00533-1

Navratilova, I., and others. 2007. Thermodynamic benchmark study using Biacore technology. Anal. Biochem. **364**: 67–77. doi:10.1016/j.ab.2007.01.031

Piliarik, M., and J. Homola. 2006. SPR sensor instrumentation, p. 95–116. *In* J. Homola and O. S. Wolfbeis [eds.], Surface plasmon resonance based sensors. Springer.

Sereda, A., J. Moreau, M. Canva, and E. Maillart. 2014. High performance multi-spectral interrogation for surface plasmon resonance imaging sensors. Biosens. Bioelectron. **54**: 175–180. doi:10.1016/j.bios.2013.10.049

Stevens, R. C., and others. 2007. Detection of the toxin domoic acid from clam extracts using a portable surface plasmon resonance biosensor. Harmful Algae **6**: 166–174. doi:10.1016/j.hal.2006.08.001

Trainer, V. L., W. P. Cochlan, A. Erickson, B. D. Bill, F. H. Cox, J. A. Borchert, and K. A. Lefebvre. 2007. Recent domoic acid closures of shellfish harvest areas in Washington State inland waterways. Harmful Algae **6**: 449–459. doi:10.1016/j.hal.2006.12.001

Trainer, V. L., and others. 2009. An ecological study of a massive bloom of toxigenic *Pseudo-nitzschia cuspidata* off the Washington State coast. Limnol. Oceanogr. **54**: 1461–1474. doi:10.4319/lo.2009.54.5.1461

Trainer, V. L., S. S. Bates, N. Lundholm, A. E. Thessen, W. P. Cochlan, N. G. Adams, and C. G. Trick. 2012. *Pseudo-nitzschia* physiological ecology, phylogeny, toxicity, monitoring and impacts on ecosystem health. Harmful Algae **14**: 271–300. doi:10.1016/j.hal.2011.10.025

Traynor, I. M., L. Plumpton, T. L. Fodey, C. Higgins, and C. Elliott. 2006. Immunobiosensor detection of domoic acid as a screening test in bivalve molluscs: comparison with liquid chromatography-based analysis. J. AOAC Int. **89**: 868–872. doi: 16792088

U.S. Department of Energy (DOE). 1994. Handbook of methods for the analysis of the various parameters of the carbon dioxide system in sea water, version 2. *In* A. G. Dickson and C. Goyet [eds.], ORNL/CDIAC-74. Oak Ridge National Laboratory.

Utermöhl, von H. 1931. Neue Wege in der quantitativen Erfassung des Planktons. (Mit besondere Beriicksichtigung des Ultraplanktons). Verh. Int. Verein. Theor. Angew. Limnol. **5**: 567–595.

Vuillemin, R., and others. 2009. CHEMINI: A new *in situ* CHEmical MINIaturized analyzer. Deep Sea Res. Part I **56**: 1391–1399. doi:10.1016/j.dsr.2009.02.002

Wang, Z., K. King, J. Ramsdell, and G. Doucette. 2007. Determination of domoic acid in seawater and phytoplankton by liquid chromatography–tandem mass spectrometry. J. Chromatogr. A **1163**: 169–176. doi:10.1016/j.chroma.2007.06.054

Yu, Q. M., S. F. Chen, A. D. Taylor, J. Homola, B. Hock, and S. Y. Jiang. 2005. Detection of low-molecular-weight domoic acid using surface plasmon resonance sensor. Sens. Actuators B **107**: 193–201. doi10.1016/j.snb.2004.10.064

Acknowledgments

The authors wish to thank the Brittany Region for funding the crews of the Côte de la Manche and the Thalia. We also very much appreciate and acknowledge the kind and efficient help of Michel Lehaitre, Albert Deuff, and Jean-Yves Coail for their advice on optics, mechanics, and electronics.

Submitted 18 March 2015
Revised 15 September 2015; 4 February 2016
Accepted 18 February 2016

Associate editor: Elizabeth Minor